JACS
JOURNAL OF THE AMERICAN CHEMICAL SOCIETY

Article

pubs.acs.org/JACS

Förster Resonance Energy Transfer Switchable Self-Assembled Micellar Nanoprobe: Ratiometric Fluorescent Trapping of Endogenous H_2S Generation via Fluvastatin-Stimulated Upregulation

Chunchang Zhao,*[,†] Xiuli Zhang,[†] Kaibin Li,[†] Shaojia Zhu,[‡] Zhiqian Guo,[†] Lili Zhang,[†] Feiyi Wang,[†] Qiang Fei,[†] Sihang Luo,[†] Ping Shi,*[,‡] He Tian,[†] and Wei-Hong Zhu*[,†]

[†]Key Laboratory for Advanced Materials and Institute of Fine Chemicals, Shanghai Key Laboratory of Functional Materials Chemistry, Collaborative Innovation Center for Coal Based Energy (i-CCE), East China University of Science and Technology, Shanghai 200237, P. R. China

[‡]State Key Laboratory of Bioreactor Engineering, East China University of Science and Technology, Shanghai 200237, P. R. China

Supporting Information

ABSTRACT: H_2S produced in small amounts by mammalian cells has been identified in mediating biological signaling functions. However, the in situ trapping of endogenous H_2S generation is still handicapped by a lack of straightforward methods with high selectivity and fast response. Here, we encapsulate a semi-cyanine-BODIPY hybrid dye (**BODInD-Cl**) and its complementary energy donor (**BODIPY1**) into the hydrophobic interior of an amphiphilic copolymer (*m*PEG-DSPE), especially for building up a ratiometric fluorescent H_2S nanoprobe with extraordinarily fast response. A remarkable red-shift in the absorption band with a gap of 200 nm in the H_2S response can efficiently switch off the Förster resonance energy transfer (FRET) from **BODIPY1** to **BODInD-Cl**, subsequently recovering the donor fluorescence. Impressively, both the interior hydrophobicity of supramolecular micelles and electron-withdrawing nature of indolium unit in **BODInD-Cl** can sharply increase aromatic nucleophilic substitution with H_2S. The ratiometric strategy based on the unique self-assembled micellar aggregate **NanoBODIPY** achieves an extremely fast response, enabling in situ imaging of endogenous H_2S production and mapping its physiological and pathological consequences. Moreover, the amphiphilic copolymer renders the micellar assembly biocompatible and soluble in aqueous solution. The established FRET-switchable macromolecular envelope around **BODInD-Cl** and **BODIPY1** enables cellular uptake, and makes a breakthrough in the trapping of endogenous H_2S generation within raw264.7 macrophages upon stimulation with fluvastatin. This study manifests that cystathione γ-lyase (CSE) upregulation contributes to endogenous H_2S generation in fluvastatin-stimulated macrophages, along with a correlation between CSE/H_2S and activating Akt signaling pathway.

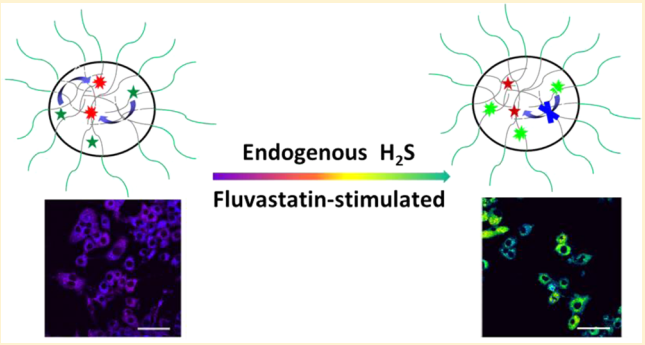

INTRODUCTION

Hydrogen sulfide (H_2S) is produced in small amounts by mammalian cells and has been identified in mediating many biological signaling functions, such as modulating blood pressure, exerting antioxidation and anti-inflammation effects, and regulating the central nervous, respiratory, and gastrointestinal system.[1−4] Endogenous H_2S can be generated enzymatically by cystathionine γ-lyase (CSE), cystathionine β-synthase (CBS), and 3-mercaptopyruvate sulfurtransferase (3-MST).[5−7] These enzymes digest cysteine or cysteine derivatives to produce H_2S within different organs and tissues.[8−10] As is well-known, abnormal H_2S production is tightly associated with a variety of human diseases, such as Alzheimer's disease and Down's syndrome.[11−13] Therefore, it is of scientific interest to develop selective methods for real-time monitoring of H_2S in living cells, mapping its physiological and pathological consequences. Fluorescence trapping with H_2S-responsive fluorescent probe offers an attractive molecular imaging technique for the in vivo detection,[14−20] mostly based on its unique chemical reactivity, such as exploiting selective H_2S-mediated reduction of azides,[21−36] trapping H_2S by proximate bis-electrophile centers,[37−43] and employing copper sulfide precipitation strategies.[44,45] However, trapping endogenous production of H_2S in living cells is still a challenge due to common problems in sensitivity, selectivity, and chemostability/photostability with currently available probes.[25] Another bottleneck encountered with most reported probes is critically limited to the response rate of H_2S.[46] Given the transient endogenous generation of H_2S in live cells, the slow response characteristic seriously retards their practical application in real-time imaging of H_2S-related biological processes.

Received: March 28, 2015
Published: June 12, 2015

DOI: 10.1021/jacs.5b03248
J. Am. Chem. Soc. 2015, 137, 8490−8498

With this in mind, we here develop a fluorescent boron dipyrromethene (BODIPY)-based platform for construction of selective and rapidly responsive H_2S probes. The design strategy relies on the thiol−halogen nucleophilic substitution of a monochlorinated boron dipyrromethene (BODIPY) core, fully employing the nucleophilic feature of H_2S. Generally, increasing the electron deficiency within the BODIPY chromophore is an effective strategy to enable aromatic nucleophilic substitution (S_NAr) proceeding more readily.[47,48] In this regard, we specifically incorporated an electron-withdrawing unit of indolium through a vinylene bridge to the BODIPY core, thus creating a semi-cyanine-BODIPY hybrid dye **BODInD-Cl** (Scheme 1). Indeed, **BODInD-Cl** realized a distinct increase in the reaction rate of thiol−halogen nucleophilic substitution, exhibiting a highly selective and fast response to H_2S. Unfortunately, its fluorescence turn-off nature leads to low signal/noise (S/N) ratios, which are detrimental to intracellular H_2S detection. Noteworthy, a remarkable red-shift up to 200 nm in absorption spectra was observed upon treatment of **BODInD-Cl** with H_2S, enabling **BODInD-Cl** as a component in Förster resonance energy transfer (FRET)-based probes, which can address the limitation in fluorescence turn-off probes.

Scheme 1. Chemical Structures of BODInD-Cl, BODIPY1, and *m*PEG-DSPE, and Formation of Micellar Aggregate NanoBODIPY for Modulation FRET from the Complementary Energy Donor (BODIPY1) to the Responsive Energy Acceptor of BODInD-Cl

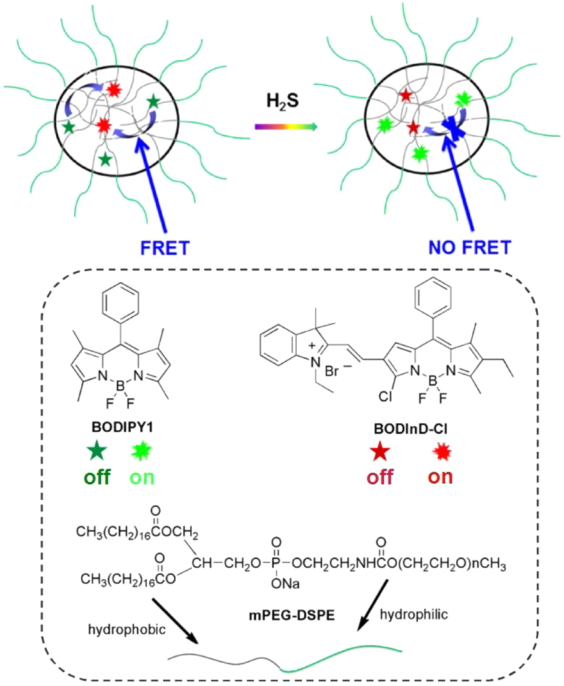

Considering that a supramolecular micelle or cluster of amphiphilic polymers can entrap multiple chromophores within the same interior of the macromolecular envelope,[49−52] we further encapsulated the semi-cyanine-BODIPY hybrid dye (**BODInD-Cl**) and its complementary energy donor (**BODIPY1**) into the hydrophobic interior of a micelle based on amphiphilic copolymer *m*PEG-DSPE (1,2-dimyristoyl-*sn*-glycero-3-phospho-ethanolamine-*N*-(methoxy(polyethylene glycol)-2000)), imposing the trapped chromophores in close proximity. In this way, the unique self-assembled micellar aggregate **NanoBODIPY** is designed to comprise **BODIPY1** as an energy donor and **BODInD-Cl** as dynamic energy acceptor due to the good spectral overlap between the emission spectrum of the donor and absorption spectrum of the acceptor, thus guaranteeing that the specific FRET from **BODIPY1** to **BODInD-Cl** occurs efficiently in the absence of H_2S (Scheme 1). In contrast, the presence of H_2S induces a remarkable shift of up to 200 nm from 540 to 738 nm in the absorption of **BODInD-Cl**, resulting in the poor overlap with the emission of **BODIPY1**, and subsequently loss of FRET with recovering the donor fluorescence. The change of FRET efficiency is reflected in an enhancement of fluorescence intensity of the donor **BODIPY1** and a decrement of that of the acceptor **BODInD-Cl**. In particular, the macromolecular envelope around **BODInD-Cl** and **BODIPY1** enables cellular uptake of living cells, which was successfully exploited for in situ ratiometric imaging of endogenous H_2S generation within raw264.7 macrophages upon stimulation with fluvastatin, a cholesterol-type drug used widely in treating cardiovascular diseases. This study demonstrates that fluvastatin-triggered CSE upregulation is responsible for the endogenous H_2S generation in macrophages. Further, a correlation between CSE/H_2S and activating Akt signaling pathway is also identified. To the best of our knowledge, the self-assembled micelle **NanoBODIPY** is the first supramolecular nanoprobe with an H_2S-triggered FRET switch, enabling the endogenous modulation of H_2S to be rapidly and accurately tracked via a ratiometric fluorescent method.

RESULTS AND DISCUSSION

Incorporating an Electron-Withdrawing Semi-Cyanine Unit for Fast Response to H_2S. The in situ trapping of endogenous H_2S generation remains handicapped by a lack of straightforward methods. Keeping in mind that H_2S is catabolized rapidly in biological systems, it is therefore highly desirable to develop specific probes with extremely fast reactivity toward H_2S for real-time monitoring of H_2S-related biological processes. Here, we exploited an approach that utilizes thiol−halogen nucleophilic substitution of a monochlorinated BODIPY. It is known that the reaction between monochlorinated BODIPY and nucleophilic reagent can be modulated via changing the electronic nature of the substituents.[47,48] Accordingly, it is possible to design an optimal probe for H_2S via modifying the electron deficient nature of BODIPY core. In our preliminary search for such a probe, we first tested our previously reported monochlorinated BODIPY (**BODIPY2**, Scheme 2). Indeed, no fluorescence response of **BODIPY2** to H_2S could be observed under physiological conditions, indicative of a lack of nucleophilic substitution tendency between the chloro group and H_2S. Because enhancement of the electron deficiency at the 3-position can increase reactivity toward nucleophiles, careful selection of an electron-withdrawing unit for appending to **BODIPY2** core would allow a judiciously designed probe for monitoring H_2S. To prove this concept, an electron-withdrawing semi-cyanine group was incorporated into the parent structure of **BODIPY2** through a vinylene unit, and **BODInD-Cl** was thus designed. As shown in Scheme 2, **BODInD-Cl** was obtained via condensation of *N*-ethyl-2,3,3-trimethylindolenine with aldehyde **BODIPY3**, which was prepared according to our previously established procedure.[53]

DOI: 10.1021/jacs.5b03248
J. Am. Chem. Soc. 2015, 137, 8490−8498

Scheme 2. Synthesis of BODInD-Cl and Proposed Reaction Mechanism with NaHS

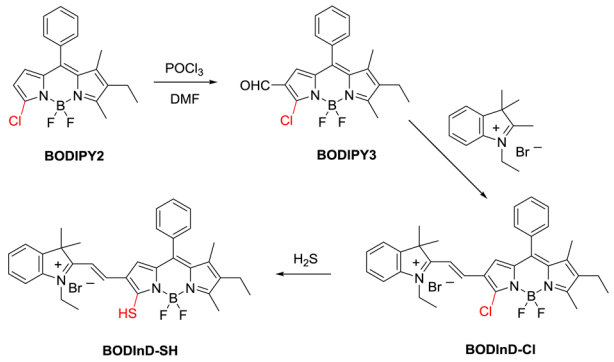

With **BODInD-Cl** in hand, we then evaluated the spectroscopic responses of **BODInD-Cl** toward H_2S under model conditions (acetonitrile/PBS buffer, 1:1, v/v, 20 mM, pH 7.4, 37 °C) by monitoring the changes in absorption and emission spectra. Here, acetonitrile was chosen as cosolvent to improve the aqueous solubility of **BODInD-Cl**. As expected, **BODInD-Cl** responded to H_2S very rapidly when using NaHS as a H_2S donor. Time-dependent fluorescence quenching of **BODInD-Cl** in the presence of H_2S showed that the reaction could be completed within minutes (Figure S1 in the Supporting Information (SI)). Furthermore, a fascinating feature was observed in the absorption, that is, addition of NaHS triggered a rapid red-shift from 540 to 738 nm (Figure 1a), resulting in the possible colorimetric and ratiometric detection even with the naked eye. Both high-performance liquid chromatography (HPLC) and high-resolution mass spectrometry (HRMS) experiments were carried out to confirm the reaction mechanism of **BODInD-Cl** and NaHS (Figure S2 in the SI). Upon incubation with NaHS (100 μM) in reaction buffer, **BODInD-Cl** (5 μM, HPLC retention time at 5.4 min) was converted efficiently and rapidly into **BODInD-SH** (retention time at 7.3 min). Also, the HRMS spectrum of **BODInD-Cl** solution in the presence of NaSH showed a m/z signal at 554.2772, corresponding to [**BODInD-SH**−Br]$^+$. All these data suggest the attachment of H_2S to **BODInD-Cl** by replacement of the chloro group (Scheme 2). Furthermore, **BODInD-Cl** displayed good selectivity to NaHS with minimum interference from other biologically relevant analytes in the PBS buffer (Figure 1b and Figure S3 in the SI). Here, the specific reaction with H_2S was retained even in the presence of 1 mM GSH, suggesting the high selectivity to H_2S over GSH.

Supramolecular Strategy to Construct Nanoprobes for Fast and Selective Response to H_2S. It is obvious that H_2S triggered fluorescence turn-off nature (Figure S1 in the SI) renders this probe less attractive in detection of endogenous H_2S within living cells due to the low S/N ratio. Fortunately, a remarkable red-shift in absorption spectra was observed when **BODInD-Cl** was treated with NaHS, showing a distinct gap of 200 nm (Figure 1a). This distinct gap in the absorption makes **BODInD-Cl** promising for construction of FRET-based probes, which enables analytes to be evaluated via the ratiometric change in two emission bands. It then can be envisioned that a fluorophore (energy donor) and **BODInD-Cl** (energy acceptor) can be integrated within a covalently linked skeleton to form a FRET pair. However, this covalent system requires a tedious multistep synthesis procedure. In contrast, the supramolecular assembly approach offers an opportunity to

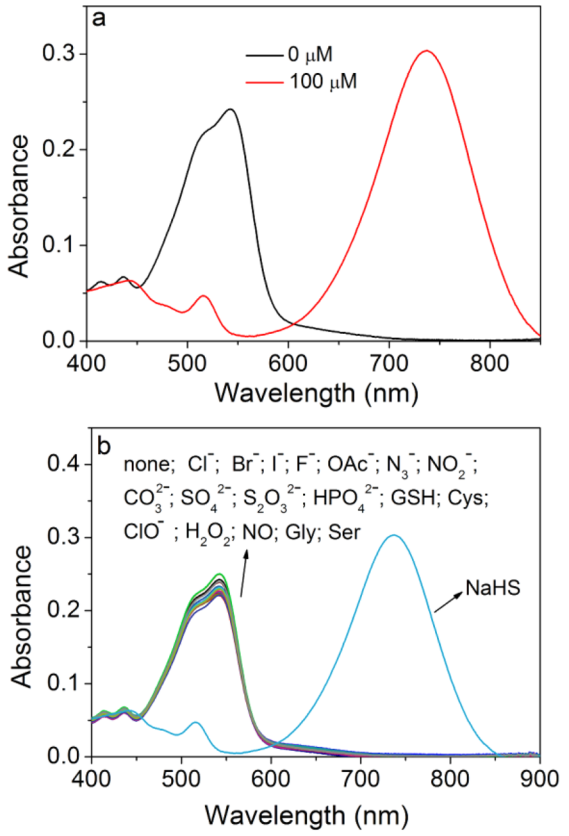

Figure 1. (a) Absorption changes of **BODInD-Cl** (5 μM) upon addition with 100 μM NaHS, and (b) changes in absorbance of **BODInD-Cl** (5 μM) in the presence of 100 μM NaHS and other biologically relevant reactive sulfur and anions (500 μM) in PBS (pH 7.4, 50% CH_3CN, v/v). Data were recorded at 30 min after addition of analytes.

overcome this limitation. Indeed, self-assembling nanoparticles of amphiphilic polymers can entrap multiple chromophores within the same interior of the macromolecular envelope, imposing the trapped chromophores in close proximity.[50−52] In this way, we can establish a specific FRET-based nanoprobe for fast and selective response to H_2S via encapsulating **BODInD-Cl** and its complementary donor in the hydrophobic part of the amphiphile.

To test this design hypothesis, we utilized an amphiphilic copolymer mPEG-DSPE as the host and **BODIPY1** as the energy donor for **BODInD-Cl** because of the good spectral overlap between the emission spectrum of the donor and absorption spectrum of the acceptor. **BODIPY1** and **BODInD-Cl** are almost insoluble in water at ambient temperature, limiting their biological applications. However, when the amphiphilic polymer mPEG-DSPE was introduced to the PBS buffer, they were readily dissolved due to the ability of this amphiphilic polymer to form hydrophilic micelles, which are capable of capturing **BODIPY1** and **BODInD-Cl** inside their hydrophobic interiors (Scheme 1). The PEG function of the formed micelles also improved the biocompatibility. The average hydrodynamic size of these micelles (named **Nano-BODIPY**) is about 10 nm as measured by dynamic light scattering and transmission electron microscopy (Figure S4 in the SI).

The absorption spectra of the micelles containing either **BODIPY1** or **BODInD-Cl** in PBS reveal the typical features of

DOI: 10.1021/jacs.5b03248
J. Am. Chem. Soc. 2015, 137, 8490−8498

BODIPY derivatives in organic solvents, with the absorption bands at 500 and 548 nm, respectively (Figure 2).

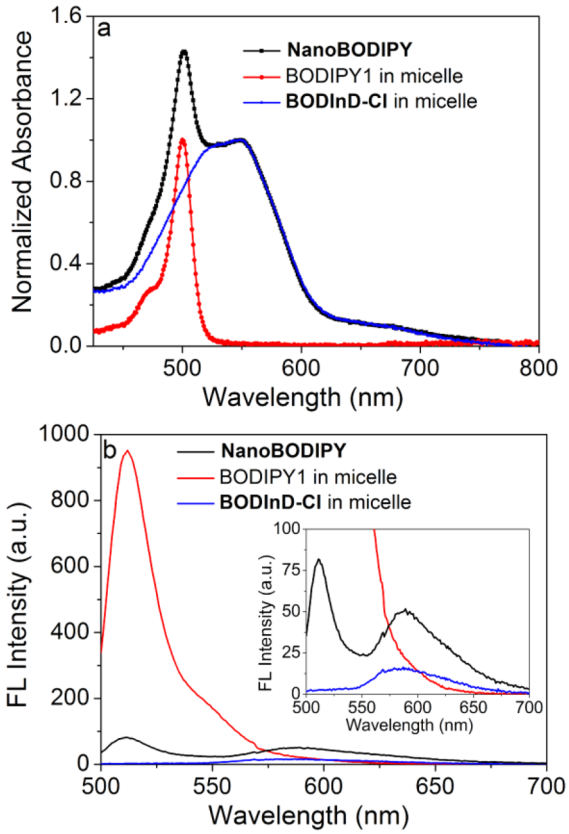

Figure 2. (a) Absorption and (b) emission spectra (λ_{ex} = 490 nm) of micelles entrapped with **BODIPY1** (1.7 μM), **BODInD-Cl** (10.0 μM), or both to form **NanoBODIPY** in PBS (pH 7.4) at 37 °C. Inset: enlargement of the fluorescence intensity between 0 and 100.

Correspondingly, the emission spectra also showed the characteristic bands at 511 and 589 nm. Notably, the emission band of **BODIPY1** is overlapped well with the absorption band of **BODInD-Cl**, suggesting that the encapsulation of both chromophores within the same micellar aggregates might result in an efficient energy transfer from **BODIPY1** to **BODInD-Cl** upon excitation of the donor **BODIPY1**.

Also, **NanoBODIPY** showed two typical absorption bands at 500 and 548 nm corresponding to those of **BODIPY1** and **BODInD-Cl**, respectively. Notably, the predominant absorption of **NanoBODIPY** is similar to that of the simple mixture of micelles containing **BODIPY1** or **BODInD-Cl** exclusively. Upon excitation at 500 or 490 nm, **NanoBODIPY** exhibited two well-resolved emission bands at 511 and 589 nm (Figure 2b). The occurrence of FRET from **BODIPY1** to **BODInD-Cl** within the micellar aggregates can be identified by comparing the spectra of **NanoBODIPY** with that of micelles containing exclusively either **BODIPY1** or **BODInD-Cl**. As can be seen from Figure 2b, the fluorescence intensity of **NanoBODIPY** at 511 nm was much weaker than that of **BODIPY1** in micelle, showing a decrease close to 90%. Compared with the fluorescence intensity of **BODInD-Cl** in micelle, significant increment of the fluorescence intensity at 589 nm was observed for **NanoBODIPY**. These data highlight the efficient occurrence of FRET. Within the interior of supramolecular micelles, the entrapped organic dyes with small Stokes shifts often show self-quenching of fluorescence behavior at relatively high local concentrations. To minimize the self-quenching among BODIPYs in **NanoBODIPY**, the optimal ratio of these dyes to *m*PEG-DSPE was evaluated as 0.0025−0.01 by weight (Figure S5 in the SI). Specifically, when 10 μM **BODInD-Cl** was used in the entrapment protocol, the FRET efficiency among the encapsulated **BODIPY1** and **BODInD-Cl** was found to be **BODIPY1** dose-dependent. Here, the optimized ratio of **BODInD-Cl** to **BODIPY1** was thus evaluated to be around 6 with the FRET efficiency up to 96% (Figure S5 in the SI). Compared with the simple mixture of **BODInD-Cl** with **BODIPY1** under the same condition, the minimal fluorescence decrement at 511 nm or enhancement at 589 nm further confirmed that the successful encapsulation of the two chromophores in close proximity contributes to efficient FRET. Given **BODInD-Cl** as a responsive energy acceptor, the presence of H_2S can lead to a remarkable red-shift with a gap of 200 nm in the absorption of **BODInD-Cl**, which would trigger poor overlap between the emission spectrum of **BODIPY1** and absorption spectrum of the acceptor, thus quickly abolishing FRET with the recovery of donor fluorescence. In this way, we can transduce the trapping of H_2S by **BODInD-Cl** from the intensity-based method in the unfavored fluorescence turn-off characteristic to the ratiometic fluorescence mode. Based on the specific FRET "on−off" sensing system, the ratiometric mode is expected to exactly allow for fast and accurate measurements with elimination of the influence in experimental conditions, such as light source, dye concentration, and background interference effects.[54−58]

The photostability of the self-assembled micellar nanoprobe was first investigated before exploiting its potential applications. Under continuous irradiation with a Hg/Xe lamp for 3 h (Figure S6 in the SI), minimal change was observed in the fluorescence intensity ratio of the two emission bands at 511 and 589 nm (I_{511}/I_{589}), indicative of excellent photostability of **NanoBODIPY**. This result suggests the superiority of the nanoprobe in bioimaging. Then, we evaluated the fluorescence responses of **NanoBODIPY** toward H_2S in aqueous solution under physiological conditions. Figure 3a and 3b show the representative fluorescence spectral changes of **NanoBODIPY** upon addition of NaHS. As expected, the addition of NaHS elicited a remarkable ratiometric fluorescence change. The emission intensity increased gradually at 511 nm with a concomitant loss of emission at 589 nm. Interestingly, this process became very fast, reaching completion within 140 s (Figure 3a). Generally, the response rate of small fluorescent **BODInD-Cl** toward H_2S, a typical nucleophilic substitution, is dependent upon the solvent polarity; for instance, the response reaction was completed from within 1000 to 4000 s when the water content increased from 50% to 80% (Figure S7 in the SI). Therefore, we can conclude that the interior hydrophobicity of supramolecular micelles from the amphiphilic copolymer can decrease the solvent interaction (polarization) with the nucleophile of H_2S, thus promoting the reaction rate between **BODInD-Cl** and H_2S. In this regard, both the interior hydrophobicity of supramolecular micelles and electron-withdrawing nature of indolium unit in **BODInD-Cl** can sharply increase aromatic nucleophilic substitution with H_2S, thus enabling H_2S to be rapidly and accurately tracked within 140 s. As a matter of fact, the response of **NanoBODIPY** is faster than that of most reported H_2S probes, which fulfill the response in the range of 30−60 min.[20,21,39] Notably, the fluorescence intensity ratio of the two emission bands at 511 and 589 nm

DOI: 10.1021/jacs.5b03248
J. Am. Chem. Soc. 2015, 137, 8490−8498

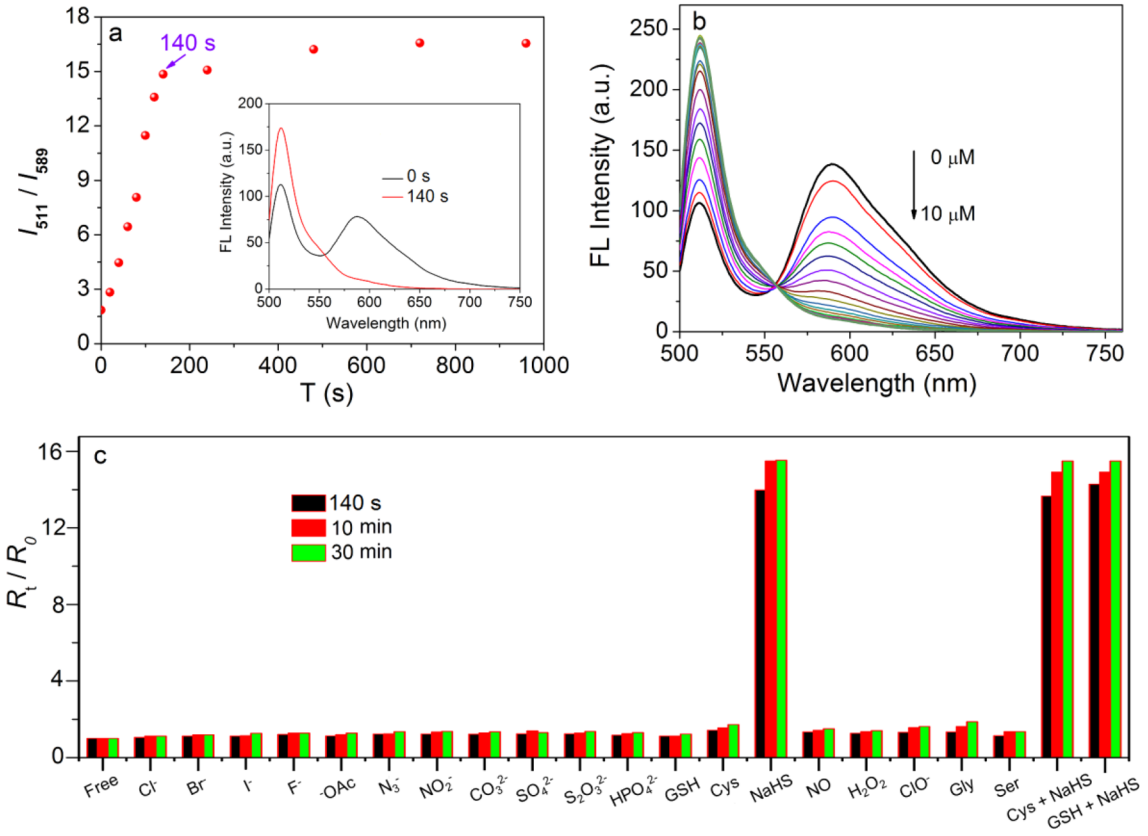

Figure 3. (a) Time-dependent ratiometric fluorescence changes of **NanoBODIPY** in the presence of NaHS (100 μM) in PBS (pH 7.4) at 37 °C, inset is changes of fluorescence spectra in the absence and presence of NaHS. (b) Fluorescence spectra of **NanoBODIPY** in the presence of various concentrations of NaHS (0, 0.5, 1.0, 1.5, 2.0, 2.5, 3.0, 3.5, 4.0, 4.5, 5.0, 5.5, 6.0, 6.5, 7.0, 7.5, 8.0, 8.5, 9.0, 9.5, 10.0 μM, respectively) in PBS buffer (pH 7.4) at 37 °C. (c) Ratiometric fluorescence changes of **NanoBODIPY** in the presence of 100 μM NaHS and other biologically relevant competing analytes in PBS (pH 7.4) at 37 °C. R_0 represents the fluorescence intensity ratio (I_{511}/I_{589}) in the absence of an analyte, and R_t represents the ratio in the presence of an analyte. Bars represent fluorescence changes 140 s, 10 min, and 30 min after addition of analytes. Data shown are for 1 mM glutathione, 1 mM cysteine, and 100 μM for other analytes. λ_{ex} = 490 nm.

(I_{511}/I_{589}) increases from 1.8 to 16.5, corresponding to a 9-fold enhancement factor, indicative of an efficient ratiometric response of **NanoBODIPY** to H_2S. Obviously, the H_2S-triggered red-shift in absorption of **BODInD-Cl** (Figure S8 in the SI) switched off the FRET process, and recovered the donor fluorescence (**BODIPY1**) at 511 nm. In addition, upon the titration of NaHS with the ratiometric fluorescence responses (Figure S9 in the SI), **NanoBODIPY** can sensitively detect submicromolar concentrations of H_2S with a detection limit of 7 nM, which is sufficiently sensitive to trap endogenous generation of H_2S in living cells.[25] Because the pH value of living cells can vary from neutral to acidic condition in different cellular compartments, experiments were carried out to interrogate pH effects on the ratiometric response of **NanoBODIPY** toward H_2S. Fortunately, it was found that pH exerted little influence on the response properties within a physiological range from pH 8 to approximately 4.5 (Figure S10 in the SI). The FRET-switchable self-assembled micellar nanoprobe of **NanoBODIPY** endows the low detection limit and fast response to H_2S within several seconds.

In good agreement with the small molecule probe **BODInD-Cl**, the micelle nanoprobe **NanoBODIPY** also showed high selectivity to H_2S over other competing analytes (Figure 3c), including reactive sulfur (RSS), oxygen (ROS), and nitrogen species (RNS). Only NaHS triggered a remarkable enhancement in the fluorescence intensity ratio (I_{511}/I_{589}), while other analytes gave minimal ratiometric changes. In addition, the ratiometric enhancement elicited by H_2S was retained even in the presence of 1 mM GSH and 1 mM Cys.

Taken together, the encapsulation of a semi-cyanine-BODIPY hybrid dye (**BODInD-Cl**) and its complementary energy donor (**BODIPY1**) into the hydrophobic interior of an amphiphilic copolymer (*m*PEG-DSPE) can realize ratiometric fluorescent sensing with rapid kinetics, enabling the trapping of endogenous H_2S production. Furthermore, the amphiphilic copolymer endows the micellar assembly with biocompatibility and aqueous solubility.

Trapping Endogenous H_2S Generation in Fluvastatin Stimulated Macrophages. After investigating the promising responsive behavior of **NanoBODIPY** toward H_2S in vitro, we then explored the ratiometric characteristic of **NanoBODIPY** for fluorescent trapping of cellular H_2S (Figure 4). Because the H_2S-producing enzyme CSE was identified as generating H_2S in macrophages, here raw264.7 macrophages were explored to interrogate the capability of **NanoBODIPY** for fluorescence imaging applications.[59] When murine raw264.7 macrophages were incubated with **NanoBODIPY** for 30 min, a bright fluorescence in the green or red channel was observed upon excitation at 488 nm. The ratio of the two emissions from green channel to red channel is about 0.8 (Figure 4A), indicative of the low level of H_2S in macrophages. Further treatment of these cells with NaHS for 30 min resulted in significant increment of

DOI: 10.1021/jacs.5b03248
J. Am. Chem. Soc. 2015, 137, 8490−8498

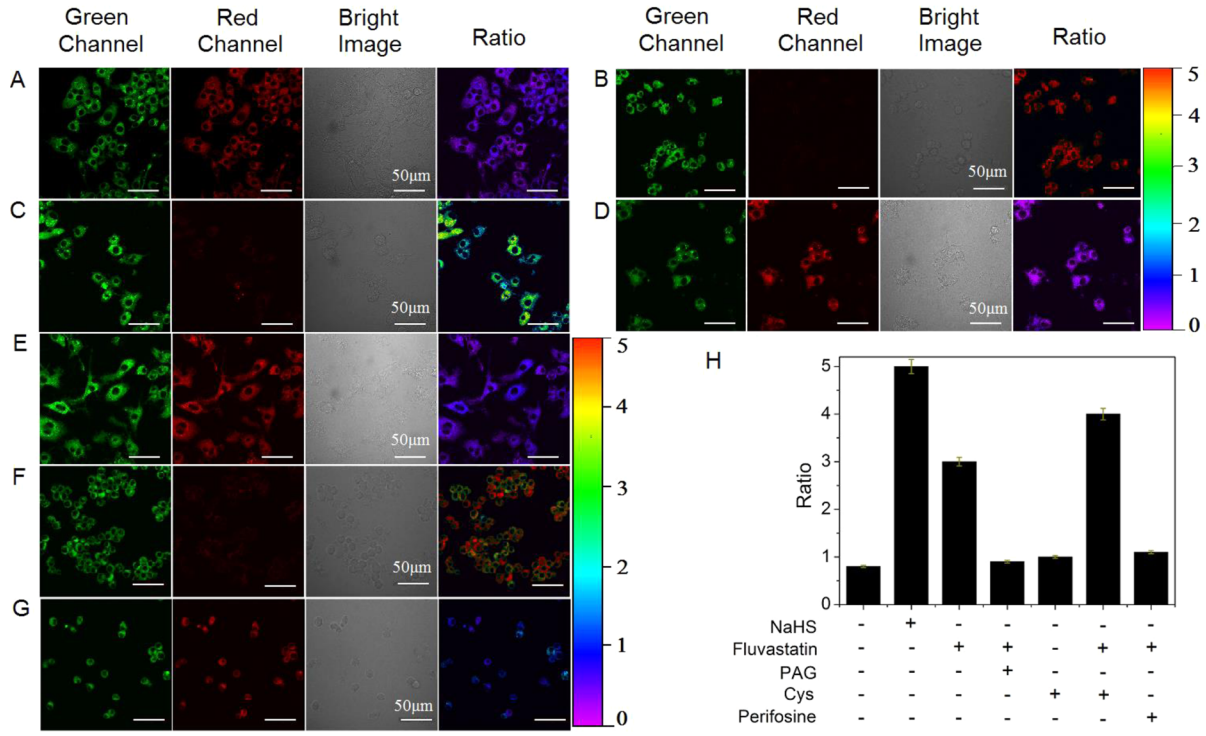

Figure 4. Confocal microscopy images of H_2S in live raw264.7 macrophages cells using **NanoBODIPY**: (A) cells incubated with **NanoBODIPY** for 30 min; (B) cells incubated with **NanoBODIPY** for 30 min, then 100 μM NaHS loaded for another 30 min; (C) cells pretreated with 2.0 μM fluvastatin for 48 h, further incubated with **NanoBODIPY** for 30 min; (D) cells pretreated with 1 mM PAG for 1 h, further incubated with 2.0 μM fluvastatin for 48 h, then incubated with **NanoBODIPY** for 30 min; (E) cells pretreated with 1 mM cysteine for 1 h, further incubated with **NanoBODIPY** for 30 min; (F) cells pretreated with 1 mM cysteine for 1 h, further incubated with 2.0 μM fluvastatin for 48 h, then incubated with **NanoBODIPY** for 30 min; (G) cells pretreated with 10 μM perifosine for 1 h, further incubated with 2.0 μM fluvastatin for 24 h, then incubated with **NanoBODIPY** for 30 min. Green channel at 500−550 nm; red channel at 560−650 nm; ratio images generated from green channel to red channel. (H) Average intensity ratios from green to red channel in fluorescence images. Data represent mean standard error.

the bright green fluorescence, accompanied by the faint red fluorescence signal (Figure 4B). A remarkable 6-fold enhancement of the emission ratio was observed. These imaging experiments indicate that **NanoBODIPY** can be used to track H_2S in dual-color imaging modality.

Next, our self-assembled nanoprobe was explored for monitoring endogenous H_2S generation with fluvastatin stimulated murine raw264.7 macrophages as a model cell system (Figure 4). Fluvastatin is a cholesterol-type drug and widely used in treating cardiovascular diseases. Recent studies have demonstrated that it stimulates the H_2S formation in raw264.7 macrophages.[59] However, the underlying molecular action mechanism of fluvastatin remains poorly understood. In this study, we employed **NanoBODIPY** to investigate the role of fluvastatin on elevating H_2S generation in raw264.7 macrophages. Macrophages cells were first incubated with fluvastatin (2.0 μM) for 48 h, and subsequently treated with **NanoBODIPY** for 30 min. H_2S generation was determined by monitoring the changes in ratiometric fluorescence signal. Compared with the untreated cells, the fluorescence ratio from green to red channel in fluvastatin-stimulated cells was increased 4-fold from 0.8 to 3.2 (Figure 4C). The fluorescence ratio was greatly decreased to 0.9 when fluvastatin-induced cells were pretreated with DL-propargylglycine (PAG, 1 mM, Figure 4D), a commercial CSE irreversible inhibitor, before incubation with **NanoBODIPY**. A marked increase of H_2S generation was noted upon introduction of cysteine (1 mM), the substrate for CSE in producing H_2S, to fluvastatin-stimulated cells (Figure 4F), with a nearly 4-fold increase in fluorescence ratio relative to that of normal cells in the presence of Cys (Figure 4E). These results manifested that fluvastatin-stimulated H_2S generation can be attributed to CSE upregulation activity in raw264.7 macrophages. Western blot analysis further demonstrated the positive effect of fluvastatin on CSE upregulation in raw264.7 macrophages. Treatment with 2.0 μM fluvastatin for 48 h stimulated a distinct elevation of CSE protein expression (Figure S11 in the SI). As a consequence, **NanoBODIPY** has been proven as a promising probe for fluorescent trapping of endogenous H_2S with the preferable ratiometric mode.

Because fluvastatin can increase the phosphorylation of Akt, it is hypothesized that the Akt signaling pathway is involved in fluvastatin-stimulated CSE upregulation and subsequent H_2S level elevation. To interrogate this process, we assayed the effects of changes in H_2S production via ratiometric florescence image in the absence and presence of Akt inhibitor, perifosine. Figure 4G displayed the distinctive reversal effect of perifosine on the elevation of H_2S elicited by fluvastatin. The fluorescence ratio was found to be significantly decreased to 1.0 when macrophages were pretreated with perifosine before incubation with fluvastatin, a 3-fold decrease relative to that in fluvastatin-stimulated cells (3.2). These imaging data imply a correlation between CSE/H_2S elevation and activating Akt signaling pathway.

As known, intracellular location of particle-based fluorophores is an important issue.[60,61] Here, the localization of **NanoBODIPY** in living cells was identified by costaining experiments using commercially available Lyso-Tracker Green, Mito-Tracker Green, and Hoechst blue, respectively (Figure 5).

DOI: 10.1021/jacs.5b03248
J. Am. Chem. Soc. 2015, 137, 8490−8498

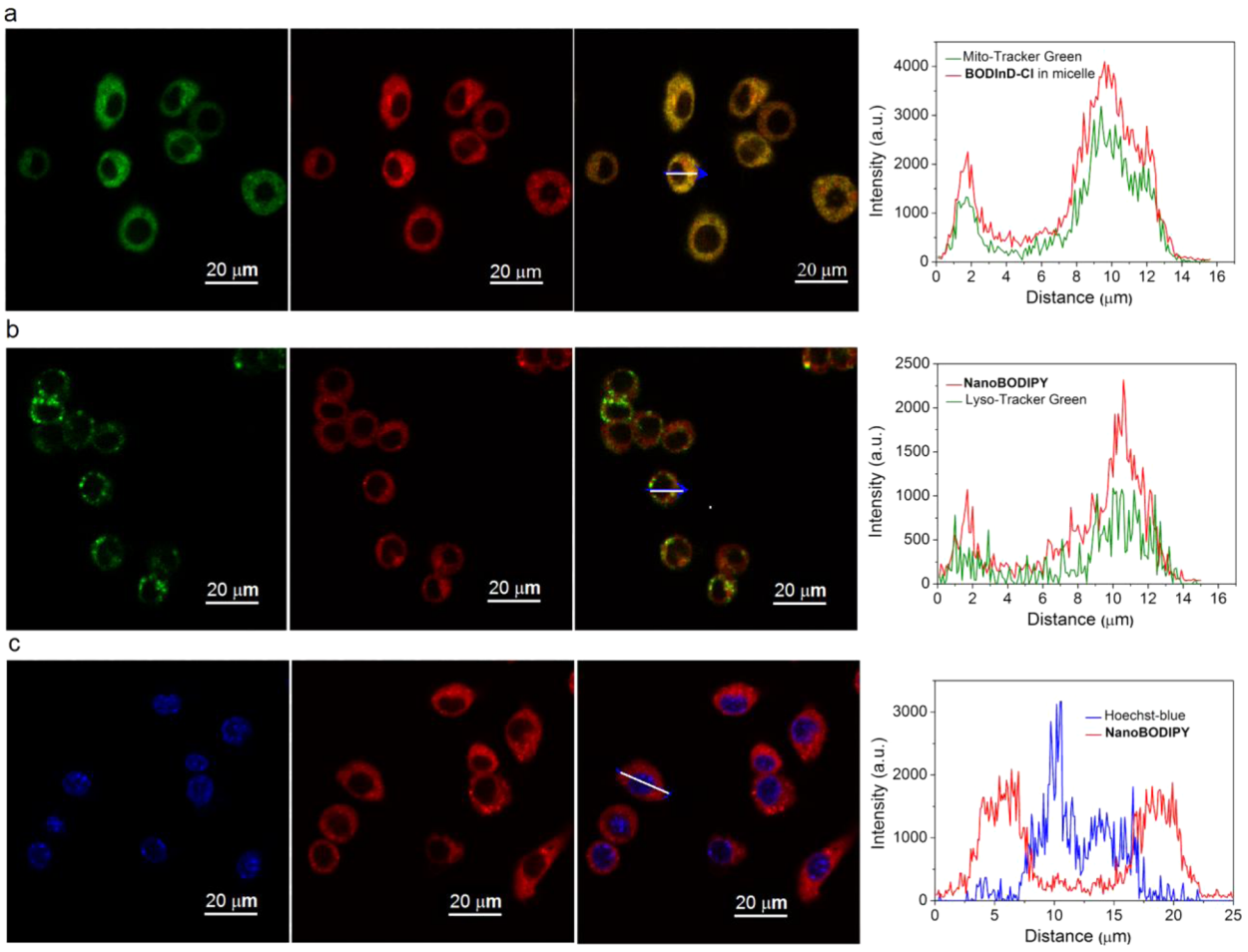

Figure 5. Confocal fluorescence images for intracellular localization of **NanoBODIPY** in cells. Cells were incubated with **NanoBODIPY** for 1 h and then costained with (a) 1 μM Lyso-Tracker Green, (b) 200 nM Mito-Tracker Green, or (c) 100 nM Hoechst for 30 min. In the case of costaining with Mito-Tracker, no commercially available tracker is suitable for colocalization with **NanoBODIPY**, thereby we here employed the strategy to encapsulate **BODInD-Cl** only within interior of supramolecular micelles, but keeping the hydrodynamic size of formed micelles similar to that of **NanoBODIPY**.

Obviously, the red fluorescence from **NanoBODIPY** colocalized well with green fluorescence from Lyso-Tracker Green or Mito-Tracker Green. A poor overlap between **NanoBODIPY** and Hoechst was also noted. Therefore, it is rational to infer that the nanoprobe is delivered to the cytoplasm with nonspecific intracellular localization.

CONCLUSIONS

In summary, we have developed a BODIPY-based platform for the construction of selective and fast responsive H_2S probes. The designed small molecular probe, **BODInD-Cl**, showed fascinating feature with a rapid red-shift in the absorption from 540 to 738 nm upon interaction with H_2S. Although the fluorescence turn-off nature renders this probe less sensitive in detection of endogenous H_2S generation within living cells, the remarkable red-shift in the absorption makes this probe promising for construction of FRET-based probes. Self-assembling micelles of amphiphilic polymers can capture multiple chromophores within the same interior of the macromolecular envelope, imposing the trapped chromophores in close proximity. By encapsulating **BODInD-Cl** and its complementary donor **BODIPY1** in the hydrophobic part of *m*PEG-DSPE, a FRET-switchable nanoprobe for fast and selective response to H_2S was established with features of aqueous solubility and biocompatibility. Both the interior hydrophobicity of supramolecular micelles and electron-withdrawing nature of indolium unit in **BODInD-Cl** can sharply increase aromatic nucleophilic substitution with H_2S, thus enabling H_2S to be rapidly and accurately tracked via a ratiometric method. Moreover, this supramolecular envelope holds promising potential in cell imaging due to several advantages such as favorable cellular uptake, aqueous solubility, biocompatibility, and ratiometric measurement, which has been successfully exploited for in situ trapping of endogenous H_2S generation within raw264.7 macrophages upon stimulation with fluvastatin. On the basis of the unique responsive energy acceptor of **BODInD-Cl**, we provide a clear clue to increasing the H_2S-response rate, building up preferable ratiometric fluorescent sensors based on the unfavored fluorescence turn-off chromophore, and making full use of the amphiphilic assembled micelles to guarantee biocompatibility and aqueous solubility. The novel nanoprobe-based platform for H_2S could be further constructed by simply employing versatile energy donors.

DOI: 10.1021/jacs.5b03248
J. Am. Chem. Soc. 2015, 137, 8490−8498

■ ASSOCIATED CONTENT

Supporting Information

Detailed characterization data, experimental procedures including preparation of **NanoBODIPY** and cell imaging, supplementary figures. The Supporting Information is available free of charge on the ACS Publications website at DOI: 10.1021/jacs.5b03248.

■ AUTHOR INFORMATION

Corresponding Authors

*zhaocchang@ecust.edu.cn
*ship@ecust.edu.cn
*whzhu@ecust.edu.cn

Notes

The authors declare no competing financial interest.

■ ACKNOWLEDGMENTS

We gratefully acknowledge the financial support by National 973 Program (2013CB733700), NSFC for Creative Research Groups (21421004) and Distinguished Young Scholars (21325625), NSFC/China, the Oriental Scholarship, the Fundamental Research Funds for the Central Universities (WJ1416005), Science and Technology Commission of Shanghai Municipality (15XD1501400), and Shanghai Scientific and Technological Innovation Project (14520720700).

■ REFERENCES

(1) Yang, G. D.; Wu, L. Y.; Jiang, B.; Yang, W.; Qi, J. S.; Cao, K.; Meng, Q. H.; Mustafa, A. K.; Mu, W. T.; Zhang, S. M.; Snyder, S. H.; Wang, R. *Science* **2008**, *322*, 587.
(2) Lefer, D. J. *Proc. Natl. Acad. Sci. U.S.A.* **2007**, *104*, 17907.
(3) Blackstone, E.; Morrison, M.; Roth, M. B. *Science* **2005**, *308*, 518.
(4) Zanardo, R. C.; Brancaleone, V.; Distrutti, E.; Fiorucci, S.; Cirino, G.; Wallace, J. L. *FASEB J.* **2006**, *20*, 2118.
(5) Kabil, O.; Banerjee, R. *J. Biol. Chem.* **2010**, *285*, 21903.
(6) Singh, S.; Padovani, D.; Leslie, R. A.; Chiku, T.; Banerjee, R. *J. Biol. Chem.* **2009**, *284*, 22457.
(7) Chiku, T.; Padovani, D.; Zhu, W.; Singh, S.; Vitvitsky, V.; Banerjee, R. *J. Biol. Chem.* **2009**, *284*, 11601.
(8) Shibuya, N.; Mikami, Y.; Kimura, Y.; Nagahara, N.; Kimura, H. *J. Biochem.* **2009**, *146*, 623.
(9) Abe, K.; Kimura, H. *J. Neurosci.* **1996**, *16*, 1066.
(10) Kamoun, P. *Amino Acids* **2004**, *26*, 243.
(11) Eto, K.; Asada, T.; Arima, K.; Makifuchi, T.; Kimura, H. *Biochem. Biophys. Res. Commun.* **2002**, *293*, 1485.
(12) Kamoun, P.; Belardinelli, M.-C.; Chabli, A.; Lallouchi, K.; Chadefaux-Vekemans, B. *Am. J. Med. Genet.* **2003**, *116A*, 310.
(13) Lee, M.; Schwab, C.; Yu, S.; McGeer, E.; McGeer, P. L. *Neurobiol. Aging* **2009**, *30*, 1523.
(14) Lin, V. S.; Chang, C. J. *Curr. Opin. Chem. Biol.* **2012**, *16*, 595.
(15) Xuan, W.; Sheng, C.; Cao, Y.; He, W.; Wang, W. *Angew. Chem., Int. Ed.* **2012**, *51*, 2282.
(16) Cao, X.; Lin, W.; Zheng, K.; He, L. *Chem. Commun.* **2012**, *48*, 10529.
(17) Yu, F.; Han, X.; Chen, L. *Chem. Commun.* **2014**, *50*, 12234.
(18) Lin, V. S.; Chen, W.; Xian, M.; Chang, C. J. *Chem. Soc. Rev.* **2015**, DOI: 10.1039/c4cs00298a.
(19) Liu, J.; Sun, Y.-Q.; Zhang, J.; Yang, T.; Cao, J.; Zhang, L.; Guo, W. *Chem. − Eur. J.* **2013**, *19*, 4717.
(20) Zhou, X.; Lee, S.; Xu, Z.; Yoon, J. *Chem. Rev.* **2015**, DOI: 10.1021/cr500567r.
(21) Lippert, A. R.; New, E. J.; Chang, C. J. *J. Am. Chem. Soc.* **2011**, *133*, 10078.
(22) Peng, H.; Cheng, Y.; Dai, C.; King, A. L.; Predmore, B. L.; Lefer, D. J.; Wang, B. *Angew. Chem., Int. Ed.* **2011**, *50*, 9672.
(23) Chen, S.; Chen, Z.-J.; Ren, W.; Ai, H.-W. *J. Am. Chem. Soc.* **2012**, *134*, 9589.
(24) Montoya, L. A.; Pluth, M. D. *Chem. Commun.* **2012**, *48*, 4767.
(25) Lina, V. S.; Lipperta, A. R.; Chang, C. J. *Proc. Natl. Acad. Sci. U.S.A.* **2013**, *110*, 7131.
(26) Bae, S. K.; Heo, C. H.; Choi, D. J.; Sen, D.; Joe, E.-H.; Cho, B. R.; Kim, H. M. *J. Am. Chem. Soc.* **2013**, *135*, 9915.
(27) Wan, Q.; Song, Y.; Li, Z.; Gao, X.; Ma, H. *Chem. Commun.* **2013**, *49*, 502.
(28) Yu, F.; Li, P.; Song, P.; Wang, B.; Zhao, J.; Han, K. *Chem. Commun.* **2012**, *48*, 2852.
(29) Das, S. K.; Lim, C. S.; Yang, S. Y.; Han, J. H.; Cho, B. R. *Chem. Commun.* **2012**, *48*, 8395.
(30) Li, X.; Yang, C.; Wu, K.; Hu, Y.; Han, Y.; Liang, S. H. *Theranostics* **2014**, *4*, 1233.
(31) Shi, D.-T.; Zhou, D.; Zang, Y.; Li, J.; Chen, G.-R.; James, T. D.; He, X.-P.; Tian, H. *Chem. Commun.* **2015**, *51*, 3653.
(32) Yu, C.; Li, X.; Zeng, F.; Zheng, F.; Wu, S. *Chem. Commun.* **2013**, *49*, 403.
(33) Wang, R.; Yu, F.; Chen, L.; Chen, H.; Wang, L.; Zhang, W. *Chem. Commun.* **2012**, *48*, 11757.
(34) Zhang, J.; Guo, W. *Chem. Commun.* **2014**, *50*, 4214.
(35) Bailey, T. S.; Pluth, M. D. *J. Am. Chem. Soc.* **2013**, *135*, 16697.
(36) Zhang, L.; Meng, W. G.; Lu, L.; Xue, Y. S.; Li, C.; Zou, F.; Liu, Y.; Zhao, J. *Sci. Rep.* **2014**, *29*, 5870.
(37) Liu, C.; Pan, J.; Li, S.; Zhao, Y.; Wu, L. Y.; Berkman, C. E.; Whorton, A. R.; Xian, M. *Angew. Chem., Int. Ed.* **2011**, *50*, 10327.
(38) Qian, Y.; Karpus, J.; Kabil, O.; Zhang, S. Y.; Zhu, H. L.; Banerjee, R.; Zhao, J.; He, C. *Nat. Commun.* **2011**, *2*, 495.
(39) Liu, C.; Peng, B.; Li, S.; Park, C.-M.; Whorton, A. R.; Xian, M. *Org. Lett.* **2012**, *14*, 2184.
(40) Liu, C.; Chen, W.; Shi, W.; Peng, B.; Zhao, Y.; Ma, H.; Xian, M. *J. Am. Chem. Soc.* **2014**, *136*, 7257.
(41) Peng, B.; Chen, W.; Liu, C.; Rosser, E. W.; Pacheco, A.; Zhao, Y.; Aguilar, H. C.; Xian, M. *Chem. − Eur. J.* **2014**, *20*, 1010.
(42) Wang, X.; Sun, J.; Zhang, W.; Ma, X.; Lv, J.; Tang, B. *Chem. Sci.* **2013**, *4*, 2551.
(43) Qian, Y.; Zhang, L.; Ding, S. T.; Deng, X.; He, C.; Zheng, X. E.; Zhu, H.-L.; Zhao, J. *Chem. Sci.* **2012**, *3*, 2920.
(44) Gu, X.; Zhu, H.; Yang, S.; Zhu, Y.-C.; Zhu, Y.-Z. *RSC Adv.* **2014**, *4*, 50097.
(45) Sasakura, K.; Hanaoka, K.; Shibuya, N.; Mikami, Y.; Kimura, Y.; Komatsu, T.; Ueno, T.; Terai, T.; Kimura, H.; Nagano, T. *J. Am. Chem. Soc.* **2011**, *133*, 18003.
(46) Chen, Y.; Zhu, C.; Yang, Z.; Chen, J.; He, Y.; Jiao, Y.; He, W.; Qiu, L.; Cen, J.; Guo, Z. *Angew. Chem., Int. Ed.* **2013**, *52*, 1688.
(47) Wang, F.; Guo, Z.; Li, X.; Li, X.; Zhao, C. *Chem.- Eur. J.* **2014**, *20*, 11471.
(48) Niu, L.-Y.; Guan, Y.-S.; Chen, Y.-Z.; Wu, L.-Z.; Tung, C.-H.; Yang, Q.-Z. *J. Am. Chem. Soc.* **2012**, *134*, 18928.
(49) Yildiz, I.; Impellizzeri, S.; Deniz, E.; McCaughan, B.; Callan, J. F.; Raymo, F. M. *J. Am. Chem. Soc.* **2011**, *133*, 871.
(50) Swaminathan, S.; Garcia-Amorós, J.; Fraix, A.; Kandoth, N.; Sortino, S.; Raymo, F. M. *Chem. Soc. Rev.* **2014**, *43*, 4167.
(51) Swaminathan, S.; Fowley, C.; McCaughan, B.; Cusido, J.; Callan, J. F.; Raymo, F. M. *J. Am. Chem. Soc.* **2014**, *136*, 7907.
(52) Hu, J. M.; Liu, S. Y. *Acc. Chem. Res.* **2014**, *47*, 2084.
(53) Zhao, C. C.; Zhang, J. X.; Wang, X. Z.; Zhang, Y. F. *Org. Biomol. Chem.* **2013**, *11*, 372.
(54) Lee, M. H.; Kim, J. S.; Sessler, J. L. *Chem. Soc. Rev.* **2015**, *44*, 4185−4191.
(55) Yang, Y.; Zhao, Q.; Feng, W.; Li, F. *Chem. Rev.* **2013**, *113*, 192.
(56) Anslyn, E. V. *J. Am. Chem. Soc.* **2010**, *132*, 15833.
(57) Jiang, W.; Fu, Q.; Fan, H.; Ho, J.; Wang, W. *Angew. Chem., Int. Ed.* **2007**, *46*, 8445.
(58) Bull, S. D.; Davidson, M. G.; van den Elsen, J. M. H.; Fossey, J. S.; Jenkins, A. T. A.; Jiang, Y.-B.; Kubo, Y.; Marken, F.; Sakurai, K.; Zhao, J.; James, T. D. *Acc. Chem. Res.* **2013**, *46*, 312.

DOI: 10.1021/jacs.5b03248
J. Am. Chem. Soc. 2015, 137, 8490−8498

(59) Xu, Y.; Du, H.-P.; Li, J.; Xu, R.; Wang, Y.-L.; You, S.-J.; Liu, H.; Wang, F.; Cao, Y.-J.; Liu, C.-F.; Hu, L.-F. *Pharmacol. Res.* **2014**, *87*, 18.
(60) Kantner, K.; Ashraf, S.; Carregal-Romero, S.; Carrillo-Carrion, C.; Collot, M.; del Pino, P.; Heimbrodt, W.; Jimenez de Aberasturi, D.; Kaiser, U.; Kazakova, L. I.; Lelle, M.; Martinez de Baroja, N.; Maria Montenegro, J.; Nazarenus, M.; Pelaz, B.; Peneva, K.; Rivera Gil, P.; Sabir, N.; Schneider, L. M.; Shabarchina, L. I.; Sukhorukov, G. B.; Vazquez, M.; Yang, F.; Parak, W. J. *Small* **2015**, *11*, 896.
(61) Hartmann, R.; Weidenbach, M.; Neubauer, M.; Fery, A.; Parak, W. J. *Angew. Chem., Int. Ed.* **2015**, *54*, 1365.

DOI: 10.1021/jacs.5b03248
J. Am. Chem. Soc. 2015, 137, 8490−8498